THE JOURNAL OF PHYSICAL CHEMISTRY Letters

Letter

pubs.acs.org/JPCL

Observation of Optical Chemical Shift by Precision Nuclear Spin Optical Rotation Measurements and Calculations

Junhui Shi,[†] Suvi Ikäläinen,[‡] Juha Vaara,[¶] and Michael V. Romalis*[,§]

[†]Department of Chemistry and [§]Department of Physics, Princeton University, Princeton, New Jersey, United States

[‡]Department of Chemistry, Aalto University, P.O. Box 16100, FI-00076 Finland

[¶]NMR Research Group, Department of Physics, University of Oulu, P.O. Box 3000, FI-90014 Finland

Supporting Information

ABSTRACT: Nuclear spin optical rotation (NSOR) is a recently developed technique for detection of nuclear magnetic resonance via rotation of light polarization, instead of the usual long-range magnetic fields. NSOR signals depend on hyperfine interactions with virtual optical excitations, giving new information about the nuclear chemical environment. We use a multipass optical cell to perform the first precision measurements of NSOR signals for a range of organic liquids and find clear distinction between proton signals for different compounds, in agreement with our earlier theoretical predictions. Detailed first-principles quantum mechanical NSOR calculations are found to be in agreement with the measurements.

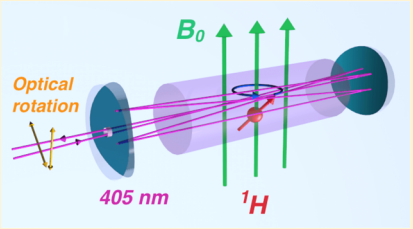

SECTION: Spectroscopy, Photochemistry, and Excited States

The effect of light on nuclear magnetic resonance (NMR) has been the subject of considerable interest as it can be used to further increase the power of NMR spectroscopy.[1,2] While NMR frequency shifts due to laser light turned out to be too small to be easily measured,[3] the inverse effect of optical rotation caused by nuclear spin polarization was observed in water and liquid ^{129}Xe.[4] The rotation of light polarization is similar to the Faraday effect caused by a nuclear magnetic field but is enhanced by the hyperfine interaction between nuclear spins and virtual electronic excitations. Recent first-principles calculations of the nuclear spin optical rotation (NSOR) predict different signals from chemically nonequivalent nuclei, opening the possibility of a new chemical analysis technique combining optical and NMR spectroscopy.[5] However, the signal-to-noise ratio (SNR) of NSOR detection has been poor in the first experiments utilizing low-field CW NMR[4] and in high-field pulsed experiments.[6,7] NSOR differences between the same nuclei in different molecular positions have not yet been clearly observed.[7] Besides ref 5, the topic of NSOR has attracted further formal theoretical[8,9] and first-principles computational[10,11] interest.

Here, we measure ^{1}H and ^{19}F NSOR with a SNR greater than 15 after 1000 s of integration and perform the first systematic NSOR measurements with an absolute uncertainty of 5%. We find that the NSOR constants V_N do not scale with the Verdet constants V of the liquids because the hyperfine interaction between electrons and nuclei is influenced by the chemical environment. The ratio of ^{1}H NSOR to Faraday rotation changes by more than a factor of 2 for the simple chemicals studied. We apply the recent first-principles theoretical method[5] for calculation of NSOR and obtain results in agreement with our measurements for both ^{1}H and ^{19}F spins.

A multipass optical cell[12,13] has a number of practical advantages for robust detection of optical rotation compared with optical cavities that have been used in the past to amplify optical dispersion effects.[14,15] It does not require locking the frequency of the laser to the optical cavity resonance or spatial mode matching of the laser beam to the cavity standing wave. It also does not require optimization of mirror reflectivity to achieve maximum power coupling into the cavity depending on losses. The multipass cell consists of two cylindrical mirrors with a small hole in one of the mirrors to let the laser beam enter and exit the cell; see Figure 1. The number of passes is determined solely by the distance between the mirrors, their curvature, and the twist angle between their axes of curvature. We adjusted the multipass cell to have 14 passes, determined by counting the number of beam spots on each mirror, with a total optical path length of 3.15 m. The laser wavelength was chosen to be 405 nm, shorter than that in previous studies, because NSOR is enhanced at short wavelengths as $1/\lambda^2$. This wavelength can be conveniently generated by a diode laser and corresponds to an absorption minimum in very pure liquids. However, the absorption is very sensitive to contamination.[16] In our measurements on water, the initial laser intensity of 8 mW was reduced to 0.4 mW after the multipass cell due to scattering by impurities; the transmission was similar for other chemicals studied. Despite significant absorption, the photon shot noise limit on the SNR is improved by the multipass cell, and overall, the SNR is greater than that in earlier studies[4,6,7] even without using a super-

Received: November 14, 2012
Accepted: January 14, 2013
Published: January 14, 2013

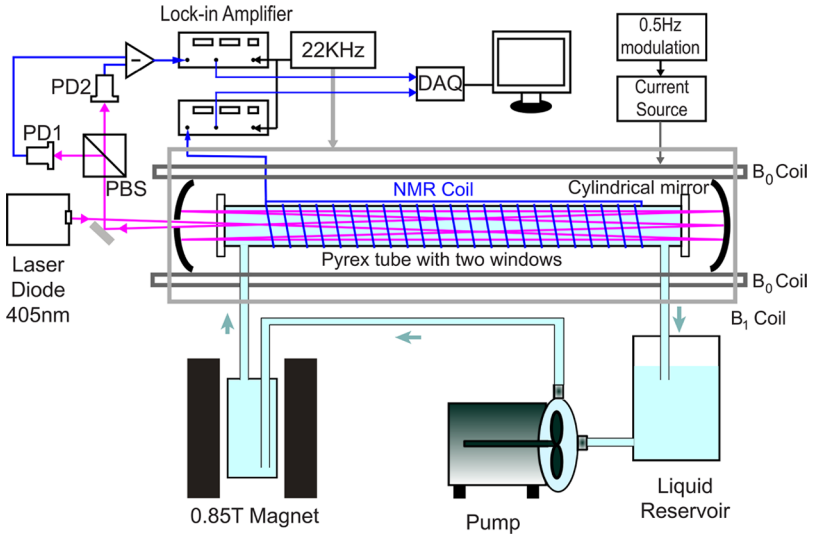

Figure 1. Apparatus for measurement of NSOR in liquids. The multipass cell consists of two cylindrical mirrors with a 40 cm separation and 50 cm radius of curvature; the sample tube is 22.5 cm long.

conducting magnet. The NSOR detection method is based on the low-field CW spin-lock technique, first developed in ref 4. As shown in Figure 1, the liquid is circulated continuously by a pump from a reservoir to a permanent prepolarizing magnet and then to a sample glass tube inside of a uniform magnetic field B_0 = 5 G, as discussed in more detail in the experimental section. An oscillating magnetic field is applied perpendicular to the B_0 field, so that the nuclear spins are adiabatically transferred to the frame rotating at the NMR frequency as they enter the region of the B_0 field. A solenoidal pick-up coil wound around the sample tube is used to measure the traditional NMR signal to determine the polarization for each flowing liquid. The optical rotation measured by a balanced polarimeter and the voltage across the pick-up coil are recorded by two lock-in amplifiers referenced to the NMR frequency. In addition, we modulate the B_0 field on and off resonance at 0.5 Hz to distinguish NMR signals from any backgrounds. For static liquids, the rotation angle noise is limited by photon shot noise, but it increases by about a factor of 2 during flow, likely due to small bubbles in the liquid. The SNR for water is typically about 15 after 1 h, while it is larger for other chemicals studied in this Letter. The NSOR signals of ^{1}H in hexane and ^{19}F in perfluorohexane are shown in Figure 2.

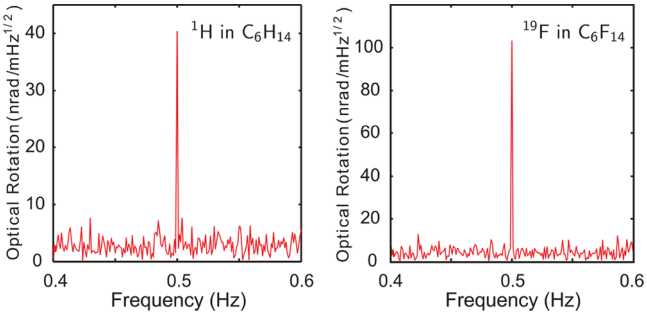

Figure 2. NSOR signal of ^{1}H in C_6H_{14} and ^{19}F in C_6F_{14} after 1000 s of integration. Because the B_0 field is modulated on and off the resonance at 0.5 Hz, the signal appears at this frequency. The SNR is about 16 and 24 for ^{1}H in C_6H_{14} and ^{19}F in C_6F_{14}, respectively.

In addition to NSOR, we also measured regular Faraday rotation in all liquids using the solenoid wound around the sample tube to create a known magnetic field. Measurements of V in a single-pass geometry revealed that they are larger by 8.3% compared to multipass geometry, likely due to small circular polarization created by multiple mirror reflections. We applied a +8.3% correction to all optical rotation data in the multipass geometry. The NSORs were measured several times for each liquid, with periodic calibration by water NSOR measurements to check the long-term stability of the apparatus. In addition to the statistical error, we assigned a systematic error of 5% to each measurement, which accounts for observed long-term changes in the signal amplitudes. We also found that our measured V are, on average, 5% smaller than literature values at 405 nm,[17−19] likely due to error in calibration of the magnetic field created by the coil wound around the cell.

The NSOR constant V_N is calculated from the NSOR angle Φ_N by dividing by the optical path length l, the molar density of nuclear spins n, and the nuclear spin polarization $P = \langle I_N \rangle / I_N$; $V_N = \Phi_{NSOR}/(nlP)$. We report our results normalized to n_A = 1 M, l = 1 cm, and fully polarized nuclei. To compare NSOR to Faraday rotation, we scale the Verdet constant by the classical magnetic field $B = \mu_0 \mu_N n_A$ generated in a long cylinder; $V_s = V\mu_0\mu_N n_A$, where μ_N is the nuclear magnetic moment. In Figure 3, we summarize our measurements of the NSOR and Verdet constants; the numerical values are given in the Supporting Information (SI). For water, the Faraday rotation accounts for all of the NSOR signal, in agreement with ref 4. For other chemicals, the NSOR constants are enhanced relative to the scaled Verdet constants by a factor greater than 2, indicating that hyperfine interactions play a large role in NSOR. The data for water, methanol, and ethanol are generally consistent with earlier first-principles theoretical calculations.[5] The enhancement of NSOR for ^{1}H bound to carbon can be explained qualitatively by smaller electronegativity of C compared with that of O. This results in greater overlap of the electronic wave function with ^{1}H in CH_2 and CH_3 groups, giving a larger hyperfine interaction.

We also measure ^{19}F NSOR in perfluorohexane, which was first observed in ref 6 at high magnetic fields. The NSOR signal after 1000 s is shown in Figure 2. The measured NSOR

dx.doi.org/10.1021/jz3018539 | J. Phys. Chem. Lett. 2013, 4, 437−441

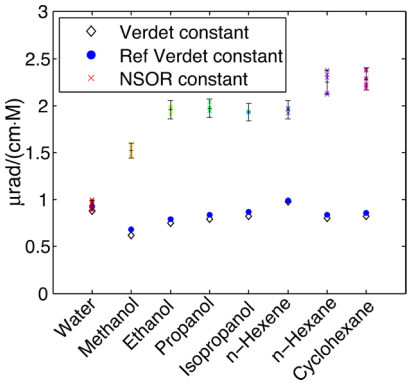

Figure 3. ^{1}H NSOR constants V_N (cross points and error bars), scaled Faraday rotation Verdet constants V_s (diamonds) from our measurements, and scaled reference Verdet constants (blue dots). All measurements of NSOR constants are shown for all chemicals to indicate the degree of experimental scatter.

constant for ^{19}F, $V_N = 13.23 \pm 0.67$ μrad/M cm, is a factor of 6 larger than that in hydrocarbons, while $V_s = 0.23$ μrad/M cm is a factor of 3.5 smaller, consistent with earlier data for V in fluorocarbons.[20] The enhancement of the NSOR signal by a factor of 57 relative to the Faraday effect is partly due to stronger hyperfine interaction in heavier atoms[4] and partly due to high electronegativity of fluorine.

The NSOR constant V_N can be calculated through the rotationally and ensemble-averaged antisymmetric polarizability[5,8,21,22]

$$V_N = -\frac{1}{2}\omega n_A c I_N \frac{e^3\hbar}{m_e}\frac{\mu_0^2}{4\pi}\gamma_N \frac{1}{6} \sum_{\varepsilon\tau\nu} \varepsilon_{\varepsilon\tau\nu}\,\mathrm{Im}\left\langle\left\langle r_\varepsilon;\, r_\tau,\, \frac{I_{N,\nu}}{r_N^3}\right\rangle\right\rangle_{\omega,0} \quad (1)$$

where ω is the frequency, I_N is the nuclear spin, γ_N is the gyromagnetic ratio, and $\varepsilon_{\varepsilon\tau\nu}$ is the Levi–Civita symbol. This expression is in terms of quadratic response theory,[23] involving a time-dependent electric dipole interaction with the light beam taken to second order (hence the appearance of components of the dipole moment, $-e\mathbf{r}$), and the static hyperfine interaction

$$H_N^{PSO} = \frac{e\hbar}{m_e}\frac{\mu_0}{4\pi}\gamma_N \mathbf{I}_N \cdot \sum_i \frac{\boldsymbol{l}_{iN}}{r_{iN}^3} \quad (2)$$

between the nuclear magnetic moment $\boldsymbol{\mu}_N = \gamma_N\hbar\mathbf{I}_N$ and the electrons, involving the electronic angular momentum about the nucleus N, $\boldsymbol{l}_N$. For heavy-atom systems such as liquid Xe, relativistic formulation should be employed.[10] In the present systems, the nonrelativistic form (eq 1) is sufficient.

Equation 1 does not include the long-range magnetic interactions between molecules, as discussed in ref 9. For a cylindrical sample, the long-range part of the classical magnetic field equals $B = (1/3)\mu_0\mu_N n_A$, resulting in an additional Faraday rotation. Hence, a bulk intermolecular correction V_B given by

$$V_B = \frac{1}{3} n_A \mu_0 \mu_N V \quad (3)$$

should be added to V_N to be fully comparable to the experimental results. We refer to the Computational Methods section for the details of the calculations.

Figure 4 and Table S1 in the SI show the calculated NSOR. Weighted averages over all ^{1}H and ^{19}F nuclei of the molecules

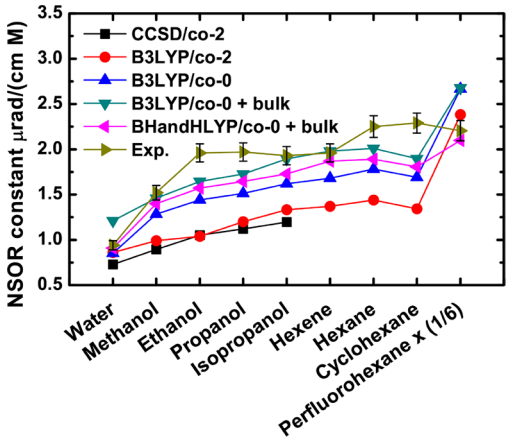

Figure 4. V_N for all molecules at the B3LYP/co-2 and B3LYP/co-0 levels of theory as well as V_N with the bulk (intermolecular) correction for B3LYP/co-0 and BHandHLYP/co-0. CCSD/co-2 data are given for the smaller molecules. Experimental values with error limits are also shown. Results for perfluorohexane are divided by a factor of 6.

are reported. Furthermore, tables of V_N for the separate chemical groups are provided in the SI. In most cases, the use of a basis set with higher quality leads to larger V_N. The only exception is water, where no systematic change is observed. Perfluorohexane shows a difference of ~10% between the two basis sets, while for the other molecules, the percentage ranges from 20 to 50%. In all cases other than perfluorohexane, the calculated intramolecular NSOR (eq 1) is smaller than the experimental result. Adding the bulk correction V_B improves the agreement of hybrid DFT (BHandHLYP/co-0 and B3LYP/co-0) data with experiment (Figure 4), apart from the exaggerated B3LYP results for perfluorohexane and water. However, the use of BHandHLYP/co-0 for water results in a better agreement with the measurements, both due to the reduced intramolecular NSOR contribution as well as the more realistic V obtained at the BHandHLYP level (Table S12 in the SI). For the larger molecules, the experimental values are reproduced qualitatively. A detailed analysis would necessitate the incorporation of solvation and intramolecular dynamics effects via molecular dynamics simulations.[11] In the case of perfluorohexane, the known issues[24] of the present DFT functionals with the hyperfine properties of ^{19}F may contribute to the observed overestimation.

Tables S3–S11 in the SI reveal that the largest NSOR occurs in the CH_2 groups, while the hydroxyl groups display distinctly smaller values than either the methyl or methylene groups for all molecules. This supports the electronegativity argument for the relatively small V_N in water (vide supra). In perfluorohexane, however, the CF_3 group features a larger V_N than the CF_2 group. The different methylene groups in propanol and hexane as well as the axial and equatorial hydrogens in cyclohexane give similar results. Alteration in the magnitude of V_N is observed for the CH_2 groups in hexene. The values for ^{1}H in the methyl groups are rather similar for all of the molecules, with isopropanol and hexane giving slightly larger NSORs than the other systems. The V_N appropriate to the hydroxyl groups differs between the molecules, with ethanol and propanol giving very small signals. In hexene, the cis-type hydrogen shows a

dx.doi.org/10.1021/jz3018539 | J. Phys. Chem. Lett. 2013, 4, 437–441

larger rotation than the other protons situated next to the double bond.

In summary, we find that experimental NSOR signals do not scale with the Verdet constant of the chemicals studied but provide unique information about the nuclear chemical environment. A simple technique utilizing a multipass optical cell can be used to obtain signals with high SNR without a superconducting magnet. Shorter multipass cells with a larger number of passes[13] can also be placed in superconducting magnets to obtain chemical shift information. Agreement with measured data is obtained with first-principles calculations using DFT calibrated against ab initio CCSD data. Hybrid DFT with 20 or 50% exact exchange is found to produce results closest to experiment. The bulk magnetization correction described in ref 9 is important. The ^{1}HSOR is able to clearly distinguish the hydroxyl group from methyl and methylene groups. Future application of these techniques to more complicated molecules can provide unique new information about their conformation and electronic state. Nuclear magneto-optic properties such as NSOR also provide new challenges to modern electronic structure theory.

EXPERIMENTAL METHODS

To reduce optical losses in the cell, the sample tube end windows have an antireflection coating on the outside surfaces. The liquid is circulated continuously at a rate of 50 mL/sec by a pump from a reservoir to a 200 mL volume inside of a 0.85 T Hallbach prepolarizing magnet and then to a 22.5 cm long, 1.5 cm diameter sample glass tube inside of a uniform magnetic field at B_0 = 5 G. As the liquid enters the region of the constant magnetic field, an oscillating magnetic field is applied at 22 kHz with an amplitude of B_1 = 0.2 G perpendicular to the B_0 field, so that the nuclear spins are adiabatically transferred to the rotating frame at the NMR frequency. We find that the NMR signal drops by less than 30% from the beginning to the end of the tube, as determined by several small coils wound at different points of the sample. For water, the NMR signal gives a polarization of $P = 1.2 \times 10^{-5}$, corresponding to a prepolarizing field of 0.36 T, smaller than the field of the magnet due to polarization loss during flow and inhomogeneous broadening of the NMR resonance due to B_0 magnetic field gradients.

COMPUTATIONAL METHODS

Optimized geometries of the molecules were obtained with the Gaussian software[25] at the B3LYP/aug-cc-pVTZ level, while the Dalton program[26] was used for NSOR and V at 405 nm. In the latter, implementations of quadratic response functions were employed for the Hartree−Fock (HF), density functional theory (DFT), and coupled-cluster (CC) methods from refs 27−29, respectively. DFT was used to obtain results of predictive quality for larger molecules. Therefore, its performance was assessed through more accurate but also more time-consuming ab initio CC singles and doubles (CCSD) calculations for water, methanol, ethanol, propanol, and isopropanol. The DFT functionals BHandHLYP(50%), B3LYP (20%), and BLYP (0%) were used, where the percentages denote the amount of exact HF exchange admixture, which has been often seen to be the factor controlling DFT accuracy for hyperfine properties.[5,24] Novel and compact so-called completeness-optimized (co) basis sets[30] were used to furnish near-basis-set-limit results for V_N, which requires an accurate description of the electronic structure both at the nuclear sites and at the outskirts of the electron cloud. This is due to the involvement of both the magnetic hyperfine and electric dipole operators. The efficiency of co sets for magnetic properties has been verified in several studies.[5,10,11,30,31] The co-2 set (10s7p3d primitive functions for C−O; 3s1p for H) was developed in ref 31 for laser-induced ^{13}C shifts in hydrocarbons. The carbon exponents[31] are used here also for oxygen. Co-0 (C−O: 12s10p4d1f, H: 8s8p5d) was generated in ref 11 for basis-set-converged NSOR for first-row main-group systems, as calibrated by ^{1}H and ^{19}FSOR calculations for the FH molecule. To assess V_B, the Verdet constants were calculated at the BHandHLYP/co-2 and B3LYP/co-2 levels for all molecules, as well as at the CCSD/co-2 level for water, methanol, ethanol, propanol, and isopropanol (see Table S12 in the SI). V computed with the co-2 basis were combined with V_N obtained with co-0 as the former property is not as sensitive to the basis set quality as NSOR.

ASSOCIATED CONTENT

Supporting Information

Summary of experimental and computational results, optimized molecular geometries, calculated NSOR data for individual groups, and the calculated Verdet constants. This material is available free of charge via the Internet at http://pubs.acs.org.

AUTHOR INFORMATION

Corresponding Author

*E-mail: romalis@princeton.edu.

Notes

The authors declare no competing financial interest.

ACKNOWLEDGMENTS

Support has been received from NSF Grant CHE-0750191 (J.S. and M.R.), the Tauno Tönning Fund (J.V.), and the Academy of Finland (S.I. and J.V.). CSC (Espoo, Finland) provided the computational facilities.

REFERENCES

(1) Warren, W. S.; Mayr, S.; Goswami, D.; West, A. P. Laser Enhanced NMR Spectroscopy. *Science* **1992**, *255*, 1683−1685.
(2) Buckingham, A.; Parlett, L. C. High-Resolution Nuclear Magnetic Resonance Spectroscopy in a Circularly Polarized Laser Beam. *Science* **1994**, *264*, 1748−50.
(3) Warren, W.; Goswami, D.; Mayr, S. Laser Enhanced NMR Spectroscopy, Revisited. *Mol. Phys.* **1998**, *93*, 371−375.
(4) Savukov, I. M.; Lee, S. K.; Romalis, M. V. Optical Detection of Liquid-State NMR. *Nature* **2006**, *442*, 1021−1024.
(5) Ikäläinen, S.; Romalis, M. V.; Lantto, P.; Vaara, J. Chemical Distinction by Nuclear Spin Optical Rotation. *Phys. Rev. Lett.* **2010**, *105*, 153001.
(6) Pagliero, D.; Dong, W.; Sakellariou, D.; Meriles, C. A. Time-Resolved, Optically Detected NMR of Fluids at High Magnetic Field. *J. Chem. Phys.* **2010**, *133*, 154505.
(7) Pagliero, D.; Meriles, C. A. Magneto-Optical Contrast in Liquid-State Optically Detected NMR Spectroscopy. *Proc. Natl. Acad. Sci. U.S.A.* **2011**, *108*, 19510−19515.
(8) Lu, T.; He, M.; Chen, D.; He, T.; Liu, F.-c. Nuclear-Spin-Induced Optical Cotton-Mouton Effect in Fluids. *Chem. Phys. Lett.* **2009**, *479*, 14−19.
(9) Yao, G.-h.; He, M.; Chen, D.-m.; He, T.-j.; Liu, F.-c. Analytical Theory of the Nuclear-Spin-Induced Optical Rotation in Liquids. *Chem. Phys.* **2011**, *387*, 39−47.

(10) Ikäläinen, S.; Lantto, P.; Vaara, J. Fully Relativistic Calculations of Faraday and Nuclear Spin-Induced Optical Rotation in Xenon. *J. Chem. Theory Comput.* **2012**, *8*, 91−98.
(11) Pennanen, T. S.; Ikäläinen, S.; Lantto, P.; Vaara, J. Nuclear Spin Optical Rotation and Faraday Effect in Gaseous and Liquid Water. *J. Chem. Phys.* **2012**, *136*, 184502.
(12) Silver, J. A. Simple Dense-Pattern Optical Multipass Cells. *Appl. Opt.* **2005**, *44*, 6545−6556.
(13) Li, S.; Vachaspati, P.; Sheng, D.; Dural, N.; Romalis, M. V. Optical Rotation in Excess of 100 rad Generated by Rb Vapor in a Multipass Cell. *Phys. Rev. A* **2011**, *84*, 061403.
(14) Zavattini, E.; et al. New PVLAS Results and Limits on Magnetically Induced Optical Rotation and Ellipticity in Vacuum. *Phys. Rev. D* **2008**, *77*, 032006.
(15) Pagliero, D.; Li, Y.; Fisher, S.; Meriles, C. A. Approach to High-Frequency, Cavity-Enhanced Faraday Rotation in Fluids. *Appl. Opt.* **2011**, *50*, 648−654.
(16) Pope, R. M.; Fry, E. S. Absorption Spectrum (380−700 nm) of Pure Water. II. Integrating Cavity Measurements. *Appl. Opt.* **1997**, *36*, 8710−8723.
(17) Washburn, E. International Critical Tables of Numerical Data, Physics, Chemistry and Technology(VI). McGraw Hill: New York, 1926.
(18) Foehr, E. G.; Fenske, M. R. Magneto-Optic Rotation of Hydrocarbons. *Ind. Eng. Chem.* **1949**, *41*, 1956−1966.
(19) Villaverde, A. B.; Donatti, D. A. Verdet Constant of Liquids; Measurements with a Pulsed Magnetic Field. *J. Chem. Phys.* **1979**, *71*, 4021−4024.
(20) Lagemann, R. T. The Verdet Constant of Certain Liquid Fluorocarbons. *J. Am. Chem. Soc.* **1949**, *71*, 368−369.
(21) Buckingham, A. D.; Stephens, P. J. Magnetic Optical Activity. *Annu. Rev. Phys. Chem.* **1966**, *17*, 399−432.
(22) Buckingham, A. D.; Long, D. A. Polarizability and Hyperpolarizability. *Philos. Trans. R. Soc. London, Ser. A* **1979**, *293*, 239−248.
(23) Olsen, J.; Jørgensen, P. Linear and Nonlinear Response Functions for an Exact State and for an MCSCF State. *J. Chem. Phys.* **1985**, *82*, 3235−3264.
(24) Vaara, J. Theory and Computation of Nuclear Magnetic Resonance Parameters. *Phys. Chem. Phys. Chem. Phys.* **2007**, *9*, 5399−5418.
(25) Frisch, M. J.; Trucks, G. W.; Schlegel, H. B.; et al. *Gaussian 03*; Gaussian, Inc.: Wallingford, CT, 2004.
(26) *DALTON2011*, A Molecular Electronic Structure Program. http://www.daltonprogram.org (2011).
(27) Hettema, H.; Jensen, H. J. Aa.; Jørgensen, P.; Olsen, J. Quadratic Response Functions for a Multiconfigurational Self-Consistent Field Wave Function. *J. Chem. Phys.* **1992**, *97*, 1174−1190.
(28) Sałek, P.; Vahtras, O.; Helgaker, T.; Ågren, H. Density-Functional Theory of Linear and Nonlinear Time-Dependent Molecular Properties. *J. Chem. Phys.* **2002**, *117*, 9630−9645.
(29) Hättig, C.; Christiansen, O.; Koch, H.; Jørgensen, P. Frequency-Dependent First Hyperpolarizabilities Using Coupled Cluster Quadratic Response Theory. *Chem. Phys. Lett.* **1997**, *269*, 428−434.
(30) Manninen, P.; Vaara, J. Systematic Gaussian Basis-Set Limit Using Completeness-Optimized Primitive Sets. A Case for Magnetic Properties. *J. Comput. Chem.* **2006**, *27*, 434−445.
(31) Ikäläinen, S.; Lantto, P.; Manninen, P.; Vaara, J. Laser-Induced Nuclear Magnetic Resonance Splitting in Hydrocarbons. *J. Chem. Phys.* **2008**, *129*, 124102.